Hidden phase in parent Fe-pnictide superconductors

Khadiza Ali,[1] Ganesh Adhikary,[2] Sangeeta Thakur,[3] Swapnil Patil,[1,4] Sanjoy K. Mahatha,[5] A. Thamizhavel,[1] Giovanni De Ninno,[2,3] Paolo Moras,[5] Polina M. Sheverdyaeva,[5] Carlo Carbone,[5] Luca Petaccia,[3] and Kalobaran Maiti[1,*]

[1]*Department of Condensed Matter Physics and Materials Science, Tata Institute of Fundamental Research, Homi Bhabha Road, Colaba, Mumbai 400005, India*

[2]*Laboratory of Quantum Optics, University of Nova Gorica, 5001 Nova Gorica, Slovenia*

[3]*Elettra Sincrotrone Trieste, Strada Statale 14 Km 163.5, I-34149 Trieste, Italy*

[4]*Department of Physics, Indian Institute of Technology (Banaras Hindu University), Varanasi 221005, India*

[5]*Istituto di Struttura della Materia, Consiglio Nazionale delle Ricerche, Area Science Park, I-34012 Trieste, Italy*

(Received 6 December 2017; published 9 February 2018)

We investigate the origin of exoticity in Fe-based systems via studying the fermiology of $CaFe_2As_2$ employing angle-resolved photoemission spectroscopy. While the Fermi surfaces (FSs) at 200 K and 31 K are observed to exhibit two-dimensional and three-dimensional (3D) topology, respectively, the FSs at intermediate temperatures reveal the emergence of the 3D topology at a temperature much lower than the structural and magnetic phase transition temperature (170 K, for the sample under scrutiny). This leads to the conclusion that the evolution of FS topology is not directly driven by the structural transition. In addition, we discover the existence in ambient conditions of energy bands related to the cT phase. These bands are distinctly resolved in the high-photon energy spectra exhibiting strong Fe 3*d* character. They gradually move to higher binding energies due to thermal compression with cooling, leading to the emergence of 3D topology in the Fermi surface. These results reveal the so-far hidden existence of a cT phase under ambient conditions, which is argued to lead to quantum fluctuations responsible for the exotic electronic properties in Fe-pnictide superconductors.

DOI: 10.1103/PhysRevB.97.054505

I. INTRODUCTION

The parent compounds of Fe-based superconductors are paramagnetic metals and undergo structural and magnetic transitions exhibiting a spin density wave (SDW) state as the magnetic ground state [1] with Fe atoms possessing magnetic moments close to a Bohr magneton [2–6]. These materials exhibit varied unusual phenomena involving competing interactions related to magnetic order, superconductivity [7,8], etc. Superconductivity in the Fe-based compounds is believed to appear due to spin fluctuations. Recent studies, however, have revealed mysterious superconductivity in pressure-induced nonmagnetic phase [9].

The finding of superconductivity under pressure raises concern over the applicability of the spin-fluctuation theory of superconductivity [10,11]. $CaFe_2As_2$ is an archetypical test case for the investigation of such puzzles. It has paramagnetic tetragonal structure at room temperature and undergoes a transition to the orthorhombic antiferromagnetic (AFM) phase below 170 K [2–4]. Application of small pressure (>0.35 GPa) collapses the system in its tetragonal symmetry; this is called the *collapsed tetragonal* (cT) phase and it does not exhibit magnetic order [12]. Extensive studies have been carried out on this system resulting in conflicting conclusions [13,14]. Some studies find T_c as high as 45 K [15] in doped $CaFe_2As_2$ under pressure and have attributed the superconductivity to the cT phase [16,17]. Some other studies do not find superconductivity in the cT phase, which is interpreted as a support of the spin-fluctuation theory of superconductivity [18]. Evidently, the link between superconductivity, structural phase, and spin fluctuations is an outstanding issue. Here, we study the fermiology of $CaFe_2As_2$ at different temperatures and discover evidence of the cT phase hidden within the structural phase at atmospheric pressure, which plays an important role in deriving the puzzling exoticity of these materials.

II. EXPERIMENTAL DETAILS

Single crystals of $CaFe_2As_2$ were grown using a high-temperature solution growth method as described in Refs. [19,20]. The composition and structure were verified by energy dispersive analysis of *x* rays followed by *x*-ray photoemission and *x*-ray diffraction. Single crystallinity was ensured by a sharp Laue pattern. It is found that the electronic properties of Fe-based compounds often depend on the sample preparation conditions [21]. For example, $SrFe_2As_2$ shows coexisting superconductivity and ferromagnetism; the volume fraction of each phase depends on the preparation conditions, i.e., the extent of strain present in the system [22]. Therefore, we studied different pieces of single crystalline $CaFe_2As_2$ samples and found that they exhibit magnetic and structural transitions at 170 K for all the samples. Angle-resolved photoemission (ARPES) measurements were carried out at Elettra, Trieste, Italy, and TIFR, Mumbai, using a Scienta R4000 WAL electron analyzer with an energy resolution fixed at 15 meV and an angle resolution of $\approx 0.3^\circ$. The samples were cleaved *in situ* along the *ab* plane, yielding a mirrorlike

*Corresponding author: kbmaiti@tifr.res.in

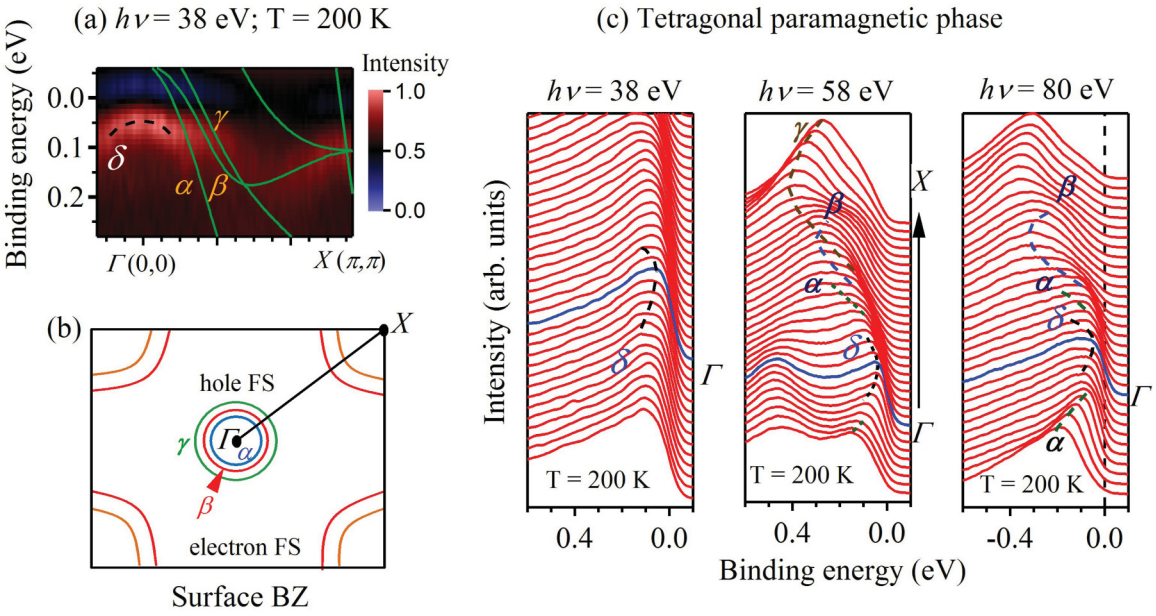

FIG. 1. ARPES results of $CaFe_2As_2$. (a) Second derivative of ARPES data at 200 K ($h\nu = 38$ eV) exhibiting three energy bands (α, β, and γ). The lines represent the *ab initio* results for the tetragonal structure after 40% compression of the energy scale. There exists one additional solid band denoted by δ around Γ. The two energy bands crossing near the X point form electron pockets. (b) Schematic of the Brillouin zone exhibiting three hole pockets around Γ corresponding to the α, β, and γ bands and electron pockets at the zone corners. (c) EDCs at 200 K with $h\nu = 38$, 58, and 80 eV exhibiting the distinct signature of the δ band in the paramagnetic tetragonal phase.

clean surface. The base pressure of the spectrometer chamber was maintained at 4×10^{-11} Torr during cleaving and the photoemission measurements. ARPES is a highly versatile and powerful tool to probe the electronic structure directly. The technique is based on photoelectric effect, which is a fast process enabling sudden approximation to capture the essential features of the experimental results. Thus, ARPES is able to capture local electronic structure at a fast time scale and is able to reveal the signature of phases hidden to other experimental techniques involving slower time scales.

III. THEORETICAL CALCULATIONS

The electronic structure calculations were carried out using the full-potential linearized augmented plane wave method as captured in the WIEN2K software [23]. In this self-consistent method, the convergence to the ground state was achieved by fixing the energy convergence criteria to 0.0001 Ry (~1 meV) using $10 \times 10 \times 10$ k points in the Brillouin zone, and for Fermi surface calculations $39 \times 39 \times 10$ k points were used. We have used the Perdew-Burke-Ernzerhof generalized gradient approximation for the density functional theoretical calculation. The Fermi surfaces were calculated using XCRYSDEN [24]. The collapsed tetragonal phase possesses the same space group but a reduced c axis and a slightly increased a axis, which leads to an overall reduction in cell volume. In the tetragonal phase (space group $I4/mmm$), the lattice parameters are $a = 3.8915$ Å, $c = 11.69$ Å, and $z_{As} = 0.372$. The orthorhombic structure of $CaFe_2As_2$ appearing at low temperature and ambient pressure has space group $Fmmm$ with the following lattice parameters: $a = 5.506$ Å, $b = 5.450$ Å, and $c = 11.664$ Å. The lattice parameters for the cT phase at $P = 0.63$ GPa are $a = 3.978$ Åand $c = 10.6073$ Å; we used $z_{As} = 0.372$ and 0.3663 for the calculations of the cT phase.

IV. RESULTS AND DISCUSSIONS

We show the ARPES data of $CaFe_2As_2$ in Fig. 1 exhibiting several energy bands and interesting evolutions. In Fig. 1(a), the ARPES data collected at 200 K (paramagnetic tetragonal phase) are superimposed with the calculated energy bands obtained by *ab initio* density functional theory. The energy scale of the theoretical results is compressed by 40% to match the experimental bandwidth; such narrowing of the local-density approximation bandwidth has been found to occur due to electron-correlation-induced effects [25,26] and is the signature of a correlated behavior of Fe $3d$ electrons in $CaFe_2As_2$. Three energy bands denoted by α, β, and γ cross the Fermi level, ϵ_F, forming three hole pockets around the Γ point [27–29]. Various ARPES studies have revealed interesting Fermi surface nesting and symmetry-broken dispersion of these bands [28,29]. Two energy bands crossing ϵ_F near the X point form electron pockets. In addition, there is a *mysterious* solid energy band just below ϵ_F at Γ, denoted by δ in the figure, which does not have a counterpart in theoretical results. The distinct signature of the δ band is observed in Fig. 1(c), where energy distribution curves (EDCs) at 200 K with photon energies ($h\nu$) of 38, 58, and 80 eV are shown. The signature of the δ band becomes well defined in the spectra obtained using higher photon energies.

The electronic structure of the magnetically ordered orthorhombic phase is discussed based on the spectra collected at 31 K. The spectra in Figs. 2(a) and 2(b) correspond to photon energies of 38 and 58 eV, which are close to $k_z = 14\pi/c$ and $16\pi/c$, respectively; the inner potential, V_0, is found to be close

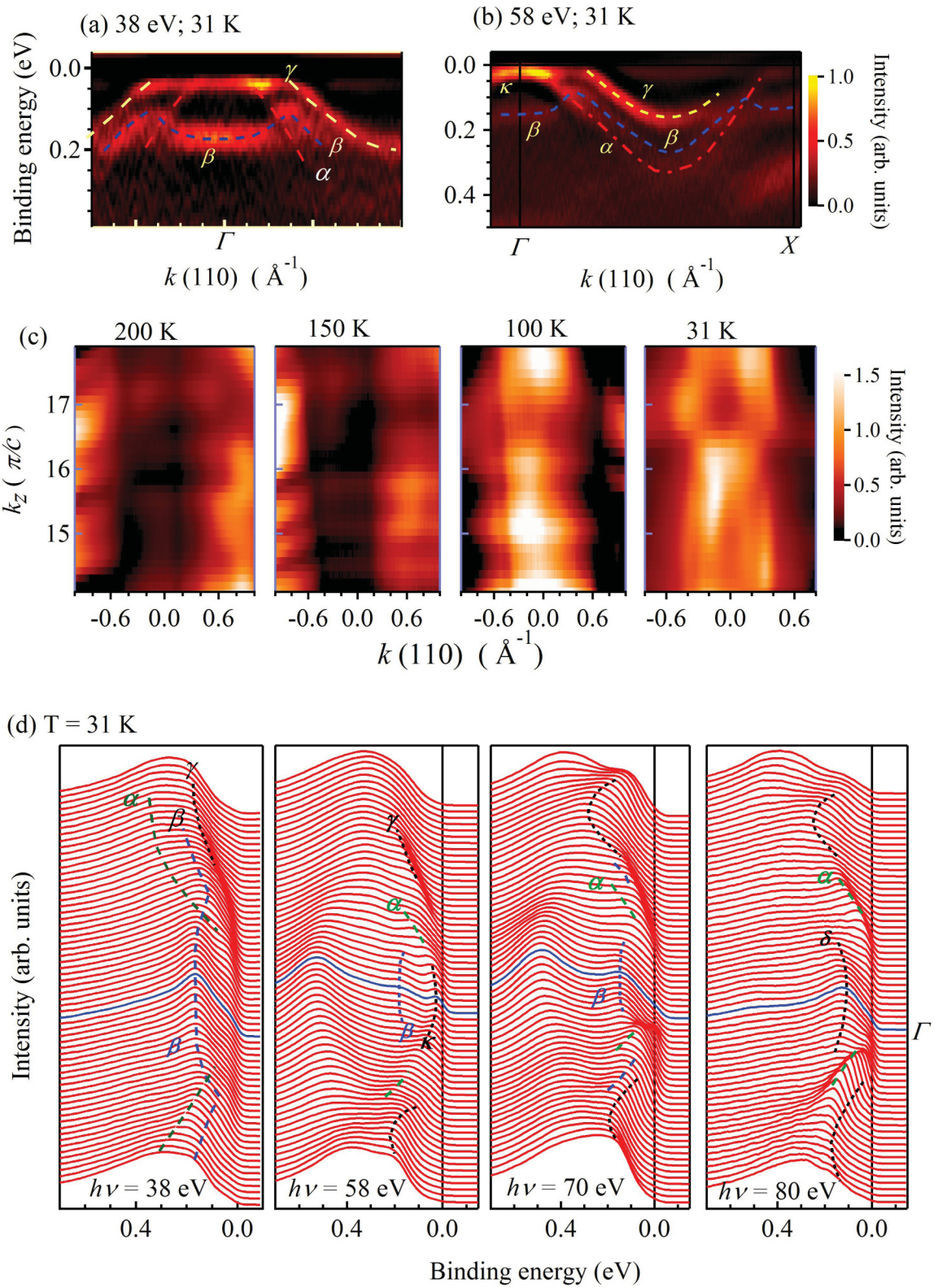

FIG. 2. Second derivative of the ARPES data collected at 31 K for (a) $h\nu = 38$ eV and (b) $h\nu = 58$ eV. The results show the distinct signature of the folded β band due to SDW transition and two hole pockets around Γ. (c) Fermi surface in the k_x-k_z plane at 200, 150, 100, and 31 K. The Fermi surface topology is two dimensional at 200 and 150 K. A k_z dependence of the Fermi surface is observed at 100 and 31 K. (d) EDCs at 31 K at $h\nu = 38$ eV ($\sim 14\pi/c$), 58 eV ($\sim 16\pi/c$), 70 eV ($\sim 17\pi/c$), and 80 eV ($\sim 18\pi/c$). α and γ bands appear to cross ϵ_F at all k_z values. EDCs collected at 58 eV exhibit an additional band below ϵ_F denoted by κ. A distinct δ band is seen in the 80-eV spectra.

to 16 eV. The spectra in both cases exhibit signatures of two hole pockets corresponding to the α and γ bands. The β band is folded (dashed line for guidance) due to the supercell symmetry formed by the AFM order [27,30]. Such band folding is also evident in Fig. 2(b); this photon energy corresponds to the Γ point on the k_z axis. The nesting of the β-band Fermi surface constituted by Fe ($3d_{xz}$, $3d_{yz}$) states and its eventual folding in the magnetically ordered phase are in line with the expectation because the Fe layers are sandwiched by As layers, and the hybridized Fe $3d$–As $4p$ states mediate the magnetic exchange coupling between the Fe $3d$ local moments. The α and γ bands cross ϵ_F in *both* the tetragonal and orthorhombic phases, which is consistent with the results obtained from the band structure calculations [31].

The evolution of the fermiology with temperatures depicted in Fig. 2(c) is surprising. At 200 K, the Fermi surface (FS) is essentially two-dimensional (2D) as expected for the tetragonal structure; this 2D topology survives even at 150 K although the system has undergone a first-order structural transition to the orthorhombic phase at 170 K. The FS at 150 K is slightly shrunk compared to the FS at 200 K. This weak effect on the Fermi surface across the structural transition is understandable as the lattice constants in the orthorhombic structure are very close to the ones in the tetragonal phase (the overall change is $< \pm 1\%$). The calculated Fermi surfaces for *both* the tetragonal and orthorhombic phases [31] corroborate well the experimental scenario observed here.

Significant change in FS topology emerges at 100 K and becomes clearly visible at 31 K. In Fig. 2(d), we show the EDCs at 31 K at $h\nu = 38$, 58, 70, and 80 eV, respectively. The distinct signature of the folded β band appears at about 180 meV at Γ. The data at $h\nu = 80$ eV exhibit an intense energy band around 120 meV akin to the δ band observed in Fig. 1 dispersing in the opposite direction of the β band. The band structure at all the k_z values shown in Fig. 2(d) exhibits two hole pockets around the k_z axis. One distinct band, named κ, appears below ϵ_F at k_z (orthorhombic phase) $\approx 16\pi/c$ ($h\nu = 58$ eV), while it is absent at other k_z data shown in the figure. This scenario was interpreted as a transition from 2D to 3D topology of the Fermi surface in the ground state [27].

If 3D topology of the Fermi surface were associated with the orthorhombic structure, the signature of the changed Fermi surface should have appeared soon after the structural transition occurring at 170 K. Experimental results exhibit a different scenario. Moreover, we discover that the emergence of the changed topology depends on the sample as shown in the Supplemental Material [32], although the structural transition occurs at the same temperature in all the cases. Thus, it appears clear that the three-dimensional character of the Fermi surface at low temperatures and the structural changes at 170 K are two different phenomena. The features near ϵ_F exhibit the intense signature of a folded β band at low photon energy spectra ($h\nu = 38$ eV) and an intense δ band at higher photon energies ($h\nu = 80$ eV). The comparison of photoemission cross sections of various electronic states indicates that the β band possesses significant As p contributions; this is expected as the magnetic long-range order occurs via intersite exchange coupling involving Fe $3d$–As $4p$ hybridized states. The δ band appears to have a predominantly Fe $3d$ character.

In Fig. 3, we show the energy bands obtained at 31 K using high photon energies, where the signature of the δ band is prominent. It is noted here that Γ in the orthorhombic and tetragonal phases under abient conditions is represented by the photon energy ~58 eV, while Γ in the cT phase corresponds to higher photon energy due to compression of the c axis. For example, Γ corresponds to $h\nu \sim 72$ eV for the structure at $P = 0.63$ GPa ($c = 10.607$ Å). While α, β, and γ bands exhibit evolution in agreement with the theory, the intense δ band is also seen below ϵ_F with the top of the band at 120-meV binding energy. This band does not shift with the change in photon energy, indicating its effective two-dimensional nature. The intensity of the feature is high at high photon energies and gradually reduces when the probing photon energy is decreased.

In Fig. 3(b), we show the EDCs corresponding to (0,0,k_z) points obtained from normal emission ARPES data at different photon energies. The distinct signature of the β band is seen at 31 K. The energy band denoted by κ (see the dashed maroon line in the figure) appears below ϵ_F near Γ on the k_z axis, indicating the absence of a corresponding Fermi surface as also seen in Fig. 2(d) ($k_z = 16\pi/c$). In the last panel of Fig. 3(b), we observe weak intensities corresponding to the β band at 200 K presumably due to the precursor effect associated with magnetic transitions often observed in various other systems [33,34]. The signature of the κ band disappears and the δ band shifts towards ϵ_F (the separation between the β and δ bands is enhanced) in the (0,0,k_z) spectra at higher temperatures. The δ band survives at 200 K and it is well discernible in the whole temperature range studied (the details of the band shifts are shown in Fig. 2 of the Supplemental Material [32]).

In order to capture the origin of these additional bands (δ and κ), we calculated the energy bands of $CaFe_2As_2$ in the cT phase with lattice constants fixed to the experimental values at pressure $P = 0.63$ GPa. The results for $z_{As} = 0.372$ (the value in the tetragonal phase) are shown in Fig. 3(c). Two of the three Fe $3d$ bands appear below ϵ_F and become degenerate at Γ; they are marked with a δ. The third one, marked with a κ, barely crosses ϵ_F close to the Γ point and gives rise to a tiny hole pocket. This is demonstrated in the Fermi surface plot in Fig. 3(d), where the κ-band hole pocket survives at Γ and exhibits weak k_z dependence. If the experimentally observed value of z_{As} ($= 0.3663$) at $P = 0.63$ GPa is used in the calculations, which corresponds to a *smaller pnictogen height* [35], even the hole pocket corresponding to the κ band moves below ϵ_F at Γ. Evidently, z_{As} is a sensitive parameter for the survival or disappearance of the Fermi surfaces leading to charge fluctuations having an important implication in the physical properties of the system. The absence of hole pockets corresponding to the δ band around Γ also affects the FS nesting resulting in a loss of magnetic order, although the Fe moments are still finite—a good scenario for quantum spin fluctuations. The δ and κ bands in the experimental results are strikingly similar to the theoretically observed energy bands of the Fermi surfaces corresponding to the cT phase possessing 3D topology.

From the above results, it is clear that, although the magnetic and structural transitions are quite similar in all the samples studied, the emergence of the k_z dependence of the Fermi

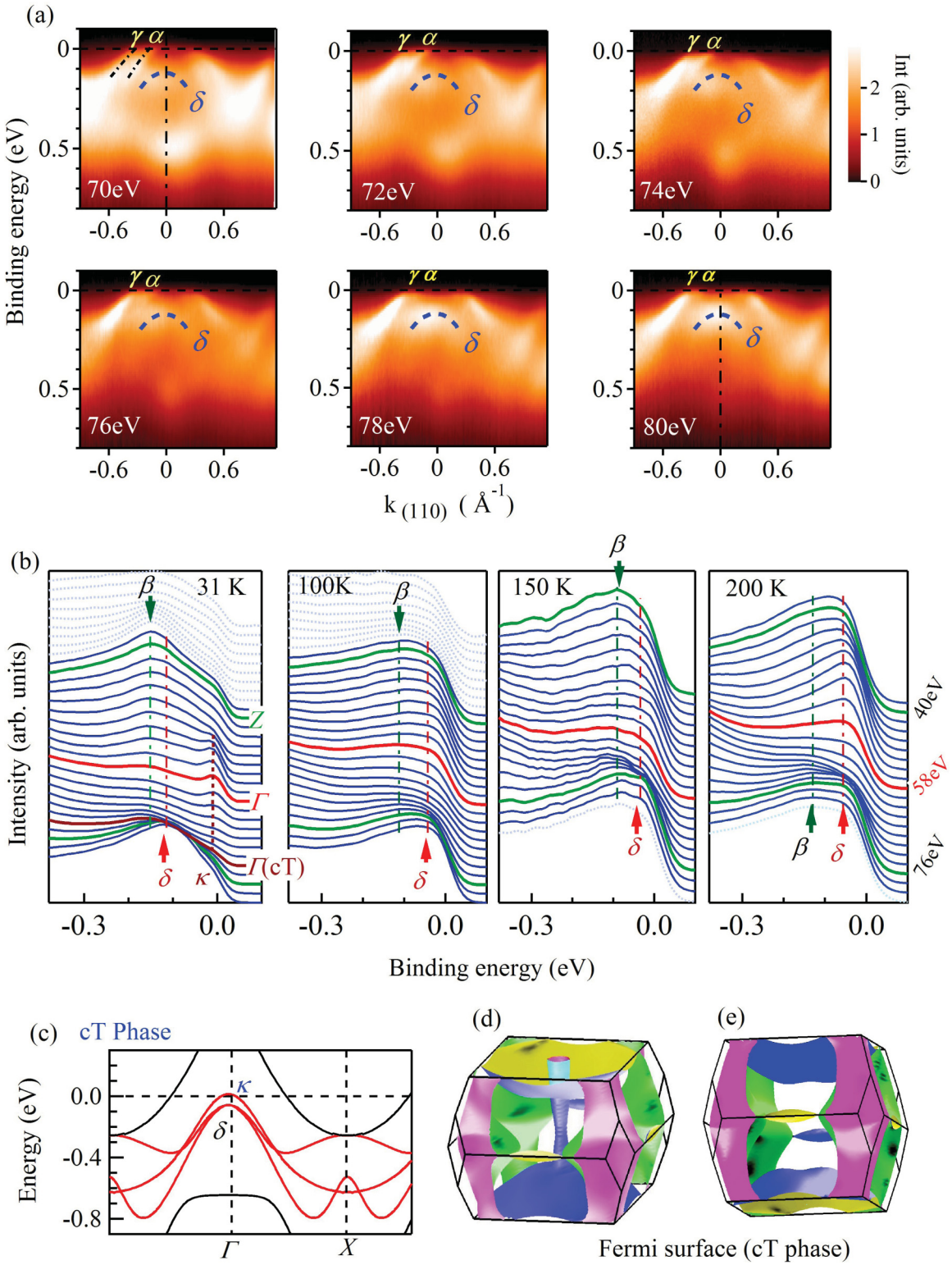

FIG. 3. (a) Energy bands at 31 K probed with different photon energies exhibiting distinct signatures of the α and γ bands crossing the Fermi level, and one additional band, δ. (b) Normal emission EDCs at 31, 100, 150, and 200 K as a function of photon energies. The red and green lines in each plot correspond to the Γ and Z points, respectively, in the orthorhombic phase. The maroon line represents the Γ point in the cT phase at $P = 0.63$ GPa (denoted by Γ(cT). Signatures of the δ and β bands are shown by vertical dashed lines. (c) Calculated energy band dispersions of $CaFe_2As_2$ in the cT phase with $z_{As} = 0.372$ (the value in tetragonal phase). Panels (d) and (e) show calculated Fermi surfaces in the cT phase with $z_{As} = 0.372$ and $z_{As} = 0.3663$, respectively (experimental value at $P = 0.63$ GPa).

surface is sample dependent. We found that better quality samples possessing sharp transitions in the bulk properties, along with bright, sharp, and well-defined Laue spots in the x-ray Laue diffraction pattern, exhibit more distinct δ and κ bands. Other samples exhibit these bands with lesser clarity presumably due to the disorder or distributed strain-induced effects. A careful look at the dispersion of the κ band in Fig. 3(b) (first panel) indicates that it does not cross ϵ_F as expected for the ambient phases; instead it moves towards higher binding energies, ∼25 meV in the 70 eV spectrum, which is the Γ(cT) point. Comparison of the experimental results and the calculated energy bands for different structural phases indicates that the δ and κ bands are an unequivocal signature of the cT phase. In the band structure calculations, we found that the converged total energy for the antiferromagnetically ordered orthorhombic $CaFe_2As_2$ is the lowest, indicating it is the ground state configuration. The converged energy for the nonmagnetic cT phase is close to the ground state energy; the calculations for all the other phases converge to higher total energies [31]. Thus, a small perturbation or strain due to the application of pressure and/or the preparation condition is expected to influence the crystal structure significantly and bring the system to the cT phase. Thermal compression would enhance the strain in the samples, which explains the shift of the δ and κ bands on cooling.

Finite electron-electron Coulomb repulsion strength among Fe 3d electrons leads to band narrowing and local character of the electrons that enhance spin fluctuation in addition to their influence on charge excitations. On the other hand, strong Hund's coupling among the 3d electrons tries to align their spin moments without much influence on charge excitations and enhances spin fluctuations in the system. These competing interactions lead to significant reduction of the Fe moment from its atomic value and the ground state is a SDW state with Fe atoms possessing magnetic moments close to a Bohr magneton [3,5,6]. Superconductivity is realized in these systems via suppression of the magnetic order, which is believed to be due to spin fluctuations [10,11]. It is evident here that the intrinsic strain brings these materials towards quantum fluctuations; the proximity to vanishing hole pockets around the Γ point due to the cT phase leads to charge fluctuations as well as spin fluctuations due to the proximity of vanishing Fermi surface nesting.

V. CONCLUSIONS

The Fe-based compounds are complex presumably due to the presence of phases hidden to various experimental probes and the electronic properties are often found to be puzzling. We discover the signature of the cT phase hidden in the normal structural phase by employing ARPES, which became possible due to the detailed study of the Fermi surfaces at intermediate temperatures and the employment of high photon energies. The coexistence of the cT phase within the ambient phases enhances the quantum fluctuations in the system and may be responsible for various exotic electronic properties in these materials.

ACKNOWLEDGMENTS

K.M., K.A., and S.P. thank ICTP for providing financial support for the measurements at Elettra, Trieste. K.M. acknowledges financial assistance from the Department of Science and Technology, Government of India under the J. C. Bose Fellowship Program and the Department of Atomic Energy, Government of India, under the DAE-SRC-OI award scheme.

[1] P. Dai, Rev. Mod. Phys. **87**, 855 (2015).
[2] N. Ni, S. Nandi, A. Kreyssig, A. I. Goldman, E. D. Mun, S. L. Bud'ko, and P. C. Canfield, Phys. Rev. B **78**, 014523 (2008).
[3] A. I. Goldman, D. N. Argyriou, B. Ouladdiaf, T. Chatterji, A. Kreyssig, S. Nandi, N. Ni, S. L. Bud'ko, P. C. Canfield, and R. J. McQueeney, Phys. Rev. B **78**, 100506 (2008).
[4] K. Maiti, Pramana **84**, 947 (2015).
[5] Q. Huang, Y. Qiu, W. Bao, M. A. Green, J. W. Lynn, Y. C. Gasparovic, T. Wu, G. Wu, and X. H. Chen, Phys. Rev. Lett. **101**, 257003 (2008).
[6] C. de La Cruz, Q. Huang, J. W. Lynn, J. Li, W. Ratcliff, II, J. L. Zarestky, H. A. Mook, G. F. Chen, J. L. Luo, N. L. Wang, and P. Dai, Nature (London) **453**, 899 (2008).
[7] D. Parker, M. G. Vavilov, A. V. Chubukov, and I. I. Mazin, Phys. Rev. B **80**, 100508 (2009).
[8] G. Adhikary, N. Sahadev, D. Biswas, R. Bindu, N. Kumar, A. Thamizhavel, S. K. Dhar, and K. Maiti, J. Phys.: Condens. Matter **25**, 225701 (2013).
[9] Y. Mizuguchi, F. Tomioka, S. Tsuda, T. Yamaguchi, and Y. Takano, Appl. Phys. Lett. **93**, 152505 (2008).
[10] F. Wang and D.-H. Lee, Science **332**, 200 (2011).
[11] M. P. Allan, Kyungmin Lee, A. W. Rost, M. H. Fischer, F. Massee, K. Kihou, C.-H. Lee, A. Iyo, H. Eisaki, T.-M. Chuang, J. C. Davis, and Eun-Ah Kim, Nat. Phys. **11**, 177 (2015).
[12] A. I. Goldman, A. Kreyssig, K. Prokeš, D. K. Pratt, D. N. Argyriou, J. W. Lynn, S. Nandi, S. A. J. Kimber, Y. Chen, Y. B. Lee, G. Samolyuk, J. B. Leão, S. J. Poulton, S. L. Bud'ko, N. Ni, P. C. Canfield, B. N. Harmon, and R. J. McQueeney, Phys. Rev. B **79**, 024513 (2009).
[13] P. C. Canfield, S. Bud'ko, N. Ni, A. Kreyssig, A. Goldman, R. McQueeney, M. Torikachvili, D. Argyriou, G. Luke, and W. Yu, Phys. C (Amsterdam, Neth.) **469**, 404 (2009).
[14] G. Adhikary, D. Biswas, N. Sahadev, R. Bindu, N. Kumar, S. K. Dhar, A. Thamizhavel, and K. Maiti, J. Appl. Phys. **115**, 123901 (2014).
[15] K. Kudo, K. Iba, M. Takasuga, Y. Kitahama, J.-I. Matsumura, M. Danura, Y. Nogami, and M. Nohara, Sci. Rep. **3**, 1478 (2013).
[16] M. S. Torikachvili, S. L. Bud'ko, N. Ni, and P. C. Canfield, Phys. Rev. Lett. **101**, 057006 (2008).
[17] H. Lee, E. Park, T. Park, V. A. Sidorov, F. Ronning, E. D. Bauer, and J. D. Thompson, Phys. Rev. B **80**, 024519 (2009).

[18] W. Yu, A. A. Aczel, T. J. Williams, S. L. Bud'ko, N. Ni, P. C. Canfield, and G. M. Luke, Phys. Rev. B **79**, 020511 (2009).
[19] N. Kumar, R. Nagalakshmi, R. Kulkarni, P. L. Paulose, A. K. Nigam, S. K. Dhar, and A. Thamizhavel, Phys. Rev. B **79**, 012504 (2009).
[20] R. Mittal, L. Pintschovius, D. Lamago, R. Heid, K. P. Bohnen, D. Reznik, S. L. Chaplot, Y. Su, N. Kumar, S. K. Dhar, A. Thamizhavel, and Th. Brueckel, Phys. Rev. Lett. **102**, 217001 (2009).
[21] B. Saparov, C. Cantoni, M. Pan, T. C. Hogan, W. Ratcliff, II, S. D. Wilson, K. Fritsch, M. Tachibana, B. D. Gaulin, and A. S. Sefat, Sci. Rep. **4**, 4120 (2014).
[22] S. R. Saha, N. P. Butch, K. Kirshenbaum, J. Paglione, and P. Y. Zavalij, Phys. Rev. Lett. **103**, 037005 (2009).
[23] P. Blaha, K. Schwarz, G. K. H. Madsen, D. Kvasnicka, and J. Luitz, *WIEN2k: An Augmented Plane Wave Plus Local Orbitals Program for Calculating Crystal Properties* (Karlheinz Schwarz, Technische Universität Wien, Austria, 2001).
[24] A. Kokalj, Comput. Mater. Sci. **28**, 155 (2003).
[25] E. Jensen and E. W. Plummer, Phys. Rev. Lett. **55**, 1912 (1985).
[26] D. D. Sarma, N. Shanthi, S. R. Barman, N. Hamada, H. Sawada, and K. Terakura, Phys. Rev. Lett. **75**, 1126 (1995); A. van Roekeghem, P. Richard, X. Shi, S. Wu, L. Zeng, B. Saparov, Y. Ohtsubo, T. Qian, A. S. Sefat, S. Biermann, and H. Ding, Phys. Rev. B **93**, 245139 (2016).
[27] C. Liu, T. Kondo, N. Ni, A. D. Palczewski, A. Bostwick, G. D. Samolyuk, R. Khasanov, M. Shi, E. Rotenberg, S. L. Bud'ko, P. C. Canfield, and A. Kaminski, Phys. Rev. Lett. **102**, 167004 (2009).
[28] T. Kondo, R. M. Fernandes, R. Khasanov, C. Liu, A. D. Palczewski, Ni Ni, M. Shi, A. Bostwick, E. Rotenberg, J. Schmalian, S. L. Bud'ko, P. C. Canfield, and A. Kaminski, Phys. Rev. B **81**, 060507 (2010).
[29] Q. Wang, Z. Sun, E. Rotenberg, F. Ronning, E. D. Bauer, H. Lin, R. S. Markiewicz, M. Lindroos, B. Barbiellini, A. Bansil, and D. S. Dessau, Phys. Rev. B **88**, 235125 (2013).
[30] V. B. Zabolotnyy, D. S. Inosov, D. V. Evtushinsky, A. Koitzsch, A. A. Kordyuk, G. L. Sun, J. T. Park, D. Haug, V. Hinkov, A. V. Boris, C. T. Lin, M. Knupfer, A. N. Yaresko, B. Büchner, A. Varykhalov, R. Follath, and S. V. Borisenko, Nature (London) **457**, 569 (2009).
[31] K. Ali and K. Maiti, Sci. Rep. **7**, 6298 (2017).
[32] See Supplemental Material at http://link.aps.org/supplemental/10.1103/PhysRevB.97.054505 for details on present angle resolved photoemission spectroscopic results from a second piece of $CaFe_2As_2$ sample called sample 2, which possesses identical bulk properties but the electronic structure exhibits differences with the results from sample 1; in this case, the two dimensional topology of the Fermi surface survives down to 100 K. We also show the temperature evolutions of the δ band from sample 1.
[33] K. Maiti, R. S. Singh, V. R. R. Medicherla, S. Rayaprol, and E. V. Sampathkumaran, Phys. Rev. Lett. **95**, 016404 (2005).
[34] R. Bindu, K. Maiti, S. Khalid, and E. V. Sampathkumaran, Phys. Rev. B **79**, 094103 (2009).
[35] K. Kuroki, H. Usui, S. Onari, R. Arita, and H. Aoki, Phys. Rev. B **79**, 224511 (2009).